Measurement of the Proton's Electric to Magnetic Form Factor Ratio from $^1\vec{\mathrm{H}}(\vec{e}, e'p)$

C. B. Crawford,[1] A. Sindile,[2] T. Akdogan,[1] R. Alarcon,[3] W. Bertozzi,[1] E. Booth,[4] T. Botto,[1] J. Calarco,[2] B. Clasie,[1] A. DeGrush,[1] T. W. Donnelly,[1] K. Dow,[1] D. Dutta,[5] M. Farkhondeh,[1] R. Fatemi,[1] O. Filoti,[2] W. Franklin,[1] H. Gao,[5] E. Geis,[3] S. Gilad,[1] W. Haeberli,[6] D. Hasell,[1] W. Hersman,[2] M. Holtrop,[2] P. Karpius,[2] M. Kohl,[1] H. Kolster,[1] T. Lee,[2] A. Maschinot,[1] J. Matthews,[1] K. McIlhany,[7] N. Meitanis,[1] R. G. Milner,[1] R. P. Redwine,[1] J. Seely,[1] A. Shinozaki,[1] S. Širca,[1] E. Six,[3] T. Smith,[8] B. Tonguc,[3] C. Tschalaer,[1] E. Tsentalovich,[1] W. Turchinetz,[1] J. F. J. van den Brand,[9] J. van der Laan,[1] F. Wang,[1] T. Wise,[6] Y. Xiao,[1] W. Xu,[5] C. Zhang,[1] Z. Zhou,[1] V. Ziskin,[1] and T. Zwart[1]

[1]*Laboratory for Nuclear Science and Bates Linear Accelerator Center, Massachusetts Institute of Technology, Cambridge, Massachusetts 02139, USA*

[2]*University of New Hampshire, Durham, New Hampshire 03824, USA*

[3]*Arizona State University, Tempe, Arizona 85287, USA*

[4]*Boston University, Boston, Massachusetts 02215, USA*

[5]*Triangle Universities Nuclear Laboratory and Duke University, Durham, North Carolina 27708-0305*

[6]*University of Wisconsin, Madison, Wisconsin 53706, USA*

[7]*United States Naval Academy, Annapolis, Maryland 21402, USA*

[8]*Dartmouth College, Hanover, New Hampshire 03755, USA*

[9]*Vrije Universiteit and NIKHEF, Amsterdam, The Netherlands*

(Received 7 September 2006; published 30 January 2007)

We report the first precision measurement of the proton electric to magnetic form factor ratio from spin-dependent elastic scattering of longitudinally polarized electrons from a polarized hydrogen internal gas target. The measurement was performed at the MIT-Bates South Hall Ring over a range of four-momentum transfer squared Q^2 from 0.15 to 0.65 $(\mathrm{GeV}/c)^2$. Significantly improved results on the proton electric and magnetic form factors are obtained in combination with existing cross-section data on elastic electron-proton scattering in the same Q^2 region.

DOI: 10.1103/PhysRevLett.98.052301 PACS numbers: 14.20.Dh, 13.40.Gp, 24.70.+s, 25.30.Bf

Understanding hadronic structure in the nonperturbative region of quantum chromodynamics (QCD) remains challenging. The electromagnetic form factors of the nucleon are fundamental quantities sensitive to the distribution of charge and magnetization within the nucleon. At low four-momentum transfer squared Q^2, they are sensitive to the pion cloud [1–5], and provide tests of effective field theories of QCD based on chiral symmetry [6]. Lattice QCD calculations continue to make advances in techniques [7] and computing power, and tests against precise nucleon form factor data will be possible in the future. Accurate measurements of nucleon electromagnetic form factors at low Q^2 are also important for the interpretation of parity-violation electron scattering experiments [8], which probe the strange quark contribution to the nucleon electromagnetic structure.

The proton electric (G_E^p) and magnetic (G_M^p) form factors have been studied extensively in the past [9] over a wide range of Q^2 from unpolarized electron-proton (e-p) elastic scattering using the Rosenbluth (L-T) separation technique [10]. It is also interesting to study the ratio $\mu_p G_E^p/G_M^p$ as a function of Q^2, where $\mu_p \sim 2.79$ is the proton magnetic moment in units of nuclear magnetons. The observation of a Q^2 dependence in the form factor ratio would suggest different charge and current spatial distributions inside the proton. The unpolarized data are consistent with $\mu_p G_E^p/G_M^p \sim 1$ up to $Q^2 \approx 6$ $(\mathrm{GeV}/c)^2$ [11,12].

Recent advances in polarized beams, targets, and polarimetry have made possible a new class of experiments extracting $\mu_p G_E^p/G_M^p$ using double polarization observables. The spin-dependent cross section has an interference term between G_E^p and G_M^p, allowing for a direct determination of $\mu_p G_E^p/G_M^p$ from either the spin-dependent asymmetry [13] or the recoil polarization measurement [14] at a single beam energy and scattering angle. The measurement of polarization observables avoids uncertainties due to detector acceptance, efficiency, and luminosity, which are major sources of systematic errors in unpolarized experiments.

New data from polarization transfer experiments [15,16] show an intriguing behavior at higher Q^2: starting at $Q^2 \approx$ 1 $(\mathrm{GeV}/c)^2$, $\mu_p G_E^p/G_M^p$ drops linearly from approximately 1 down to 0.28 at the highest measured Q^2 value [~ 5.54 $(\mathrm{GeV}/c)^2$]. This is inconsistent with previous unpolarized results [11,12], verified by recent experiments [17,18]. While the high Q^2 data on $\mu_p G_E^p/G_M^p$ from recoil polarization experiments [15,16] have been described in terms of nonzero parton orbital angular momentum or hadron helicity flip [4,19–22], it is important to understand the discrepancy between results obtained from recoil proton polarization measurements and those from the

Rosenbluth method. Calculations of the two-photon exchange (TPE) contribution are able to explain the observed discrepancy [23]. The predicted TPE contribution has a large effect on Rosenbluth extractions, but only a minor effect on polarized experiments.

In this Letter we report the first measurement of $\mu_p G_E^p/G_M^p$ from ${}^1\vec{\mathrm{H}}(\vec{e}, e'p)$ in the Q^2 region between 0.15 and 0.65 $(\mathrm{GeV}/c)^2$ [24,25], overlapping with the lower Q^2 region of the recoil polarization data [15,26–29]. This is an important region which allows for tests of effective field theory predictions and future precision results of lattice QCD. It also helps to quantify the role of the pion cloud in the structure of the nucleon. The polarized target technique has different sources of systematic uncertainty than recoil polarimetry, but still benefits from the same cancellations in systematic uncertainties such as detection efficiency and luminosity. The ${}^1\vec{\mathrm{H}}(\vec{e}, e'p)$ asymmetry was previously measured at $Q^2 = 0.4$ $(\mathrm{GeV}/c)^2$ [30] with a precision only sufficient to extract the sign of $\mu_p G_E^p/G_M^p$, and more recently at a higher Q^2 value of 1.51 $(\mathrm{GeV}/c)^2$ [31], but without employing the super-ratio technique described below.

In the one-photon exchange approximation, the elastic scattering asymmetry of longitudinally polarized electrons from polarized protons with respect to the electron beam helicity has the form [13]

$$A_{\mathrm{phys}} = \frac{v_z \cos\theta^* G_M^{p2} + v_x \sin\theta^* \cos\phi^* G_M^p G_E^p}{(\tau G_M^{p2} + \epsilon G_E^{p2})/[\epsilon(1+\tau)]}, \quad (1)$$

where θ^* and ϕ^* are the polar and azimuthal angles of the target polarization defined relative to the three-momentum transfer vector of the virtual photon and $\tau = Q^2/(4M_p^2)$ with the proton mass M_p. The longitudinal polarization of the virtual photon is denoted as $\epsilon = [1 + 2(1 + \tau)\tan^2(\theta_e/2)]^{-1}$ where θ_e is the electron scattering angle, and $v_z = -2\tau \tan(\theta_e/2)\sqrt{1/(1+\tau) + \tan^2(\theta_e/2)}$, $v_x = -2\tan(\theta_e/2)\sqrt{\tau/(1+\tau)}$ are kinematic factors. The experimental asymmetry

$$A_{\mathrm{exp}} = P_b P_t A_{\mathrm{phys}} \quad (2)$$

is reduced by the beam (P_b) and target (P_t) polarizations.

The form factor ratio $\mu_p G_E^p/G_M^p$ and the polarization product $P_b P_t$ can be determined separately from two experimental asymmetries A_l and A_r measured simultaneously at the same Q^2 value, but with different spin orientations (θ_l^*, ϕ_l^*) and (θ_r^*, ϕ_r^*), respectively, by using a detector with left and right sectors symmetric about the incident electron beam. For a target polarization angle oriented ~45° to the left of the beam, A_l (A_r) is predominantly transverse (longitudinal).

The Bates Large Acceptance Spectrometer Toroid (BLAST) experiment was carried out in the South Hall Ring (SHR) of the MIT-Bates Linear Accelerator Center, which stored an intense polarized beam with a beam current of up to 225 mA and longitudinal electron polarization of 65%. A 180° spin rotator (Siberian snake) was used in the ring opposite the interaction point to preserve the longitudinal electron polarization at the target, which was continuously monitored with a Compton polarimeter installed upstream of the internal target region. The ring was emptied and filled every 15 minutes, alternating electron helicity on successive fills.

The electrons scattered from polarized protons in a cylindrical, windowless aluminum target tube 60 cm long by 15 mm in diameter. The polarized protons were fed from an atomic beam source (ABS) located above the target, well shielded against the strong, spatially varying magnetic field of the toroid [32]. A 10 mm diameter tungsten collimator upstream of the target protected the cell wall coating from exposure to the beam and minimized the background rate in the detector. The ABS provided highly polarized ($P_t \sim 80\%$) isotopically pure hydrogen atoms. The spin state was randomly changed every five minutes by switching the final rf transition before the target to ensure equal target intensities for both states. The average target spin direction was oriented 48.0° to the left of the beam direction using a 0.04 T holding field.

The relatively low luminosity (10^{31}–10^{32} $\mathrm{cm}^{-2}\,\mathrm{s}^{-1}$) typical with internal gas targets in storage rings required the use of a large acceptance spectrometer. The symmetric detector package was built around eight copper coils which provided a maximum 0.38 T toroidal magnetic field at 6730 A, resulting in an integrated field strength of 0.15–0.44 Tm for momentum analysis. Two of the eight sectors covering scattering angles of 23°–76° and ±15° out of plane were instrumented with: three drift chambers each for momentum, angle, and position determination of charged tracks, plastic scintillators for triggering and time-of-flight particle identification, and Čerenkov detectors for pion rejection. Details of the BLAST detector can be found in [33].

Data were acquired for a total integrated charge of 298 kC on the target. The elastic events were detected in coincidence with a hardware trigger requirement of scintillator signals for both the electron and proton. A second-level trigger additionally required signals in the wire chambers to reduce excessive trigger rates and to decrease the computer dead-time. The beam current was measured using a parametric direct current transformer in the ring.

The elastic events were selected with a cut on the invariant mass of the virtual photon and the target proton system, fiducial cuts on the polar and azimuthal acceptance, and cuts on the position of the electron and proton vertex in the target cell. These cuts were consistent with kinematic cuts on angle, momentum, and timing correlations between the scattered electron and the recoil proton, made possible by the overdetermination of the elastic reaction. The cuts were sufficient to reduce the background to less than 1.5% without significantly decreasing the

TABLE I. Experimental asymmetries A_l, A_r ± stat uncertainties with all corrections applied, and extracted proton form factor ratio $\mu_p G_E^p/G_M^p$ ± stat ± syst uncertainties.

Q^2 $(\mathrm{GeV}/c)^2$	$\langle Q^2 \rangle$	A_l	A_r	$\mu_p G_E^p/G_M^p$
0.150–0.175	0.162	-0.0837 ± 0.0015	-0.1023 ± 0.0013	$1.019 \pm 0.013 \pm 0.015$
0.175–0.211	0.191	-0.0976 ± 0.0014	-0.1213 ± 0.0014	$1.006 \pm 0.012 \pm 0.014$
0.211–0.257	0.232	-0.1178 ± 0.0017	-0.1453 ± 0.0017	$0.999 \pm 0.012 \pm 0.012$
0.257–0.314	0.282	-0.1400 ± 0.0022	-0.1772 ± 0.0020	$0.973 \pm 0.012 \pm 0.011$
0.314–0.382	0.345	-0.1730 ± 0.0026	-0.2100 ± 0.0025	$0.973 \pm 0.014 \pm 0.010$
0.382–0.461	0.419	-0.2008 ± 0.0031	-0.2400 ± 0.0033	$0.980 \pm 0.016 \pm 0.009$
0.461–0.550	0.500	-0.2337 ± 0.0039	-0.2681 ± 0.0040	$0.993 \pm 0.019 \pm 0.008$
0.550–0.650	0.591	-0.2612 ± 0.0054	-0.2999 ± 0.0057	$0.961 \pm 0.025 \pm 0.007$

elastic yield. The remaining background was measured with 14.9 kC of integrated charge on the same target cell without hydrogen flowing. Additional background rates from broadening of the beam halo due to gas in the target were found to be negligible by comparing the quasielastic $(e, e'n)$ rates between hydrogen and empty targets.

Separate yields σ_{ij} were analyzed for each combination of electron helicity i and target spin state j, normalized to the integrated beam current. They were divided into eight Q^2 bins, listed in Table I. The event-weighted $\langle Q^2 \rangle$ was formed from the average of $\langle Q_e^2 \rangle$ (determined from the electron scattering angle) and $\langle Q_p^2 \rangle$ (from the proton recoil angle) in each bin. The yield distributions were in good agreement with results from a Monte Carlo simulation, that included all detector efficiencies.

The experimental double asymmetry was formed from $(\sigma_{++} - \sigma_{+-} - \sigma_{-+} + \sigma_{--})/\Sigma\sigma_{ij}$. The beam and target single-spin asymmetries were also analyzed and served as a monitor of false asymmetries, which were found to be negligible. The experimental asymmetry was corrected for dilution by unpolarized background. Radiative corrections were also applied using the code MASCARAD [34], but were less than 0.43% for A_r and 0.16% for A_l.

To extract the form factor ratio, the experimental asymmetries A_l and A_r were interpolated in each Q^2 bin to the average value of $\langle Q^2 \rangle$ in the left and right sectors (a correction of less than 0.25%). As discussed previously, the polarization product $P_b P_t$ and the form factor ratio $\mu_p G_E^p/G_M^p$ can be determined from the measured asymmetries A_l and A_r using Eqs. (1) and (2). This way the so-called super-ratio A_l/A_r would yield $\mu_p G_E^p/G_M^p$ and $P_b P_t$ independently for each Q^2 bin. The eight values of $P_b P_t$ extracted in this manner were self-consistent. The final analysis was done with a 9-parameter fit (8 values of $\mu_p G_E^p/G_M^p$ and a single value of $P_b P_t$) to the 16 asymmetries listed in Table I for optimal extraction of the form factor ratio [24] (consistent with the super-ratio analysis), resulting in $P_b P_t = 0.537 \pm 0.003(\mathrm{stat}) \pm 0.007(\mathrm{syst})$.

The dominant source of systematic uncertainty was the determination of $\langle Q^2 \rangle$, estimated from the difference between $\langle Q_e^2 \rangle$ and $\langle Q_p^2 \rangle$ to be less than 0.002 $(\mathrm{GeV}/c)^2$. The correlation is unknown since different regions of the spectrometer were used for each Q^2 bin. The event-weighted average spin angle of the target with respect to the beam was $48.0° \pm 0.4°(\mathrm{stat}) \pm 0.3°(\mathrm{syst})$, extracted from the analysis of the T_{20} tensor analyzing power in elastic scattering from deuterium in combination with a careful mapping of the magnetic field in the target region [35]. The resulting systematic uncertainty in $\mu_p G_E^p/G_M^p$ was less than 0.35% because of reduced sensitivity to the target spin angle uncertainty due to a compensation in the simultaneous extraction of $P_b P_t$. All other systematic uncertainties including Coulomb distortion were negligible.

The results are listed in Table I and are displayed in Fig. 1 with the inner error bars due to statistical uncertainties and the outer error bars being the total (statistical and systematic contributions added in quadrature). Also shown in Fig. 1 are published recoil polarization data [15,26–29], together with a few selected models discussed in [9]: a soliton model [36], a relativistic constituent quark model (CQM) with SU(6) symmetry breaking, and a constituent quark form factor [37], an extended vector meson dominance model [38], an updated dispersion model [39], and a Lorentz covariant chiral quark model [1]. We also show the

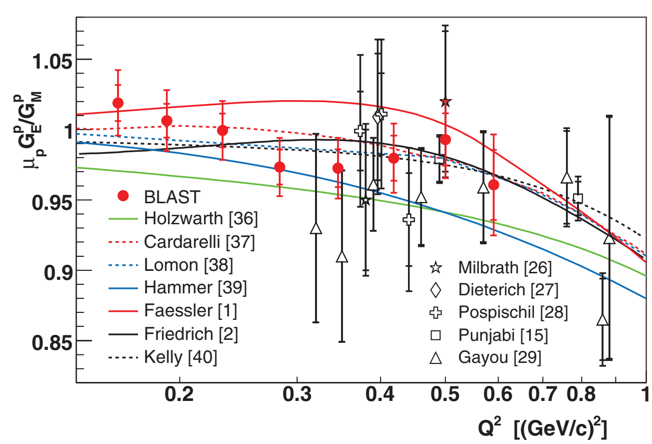

FIG. 1 (color). Results of $\mu_p G_E^p/G_M^p$ shown with the world polarized data [15,26–29] and several models [1,2,36–40] described in the text.

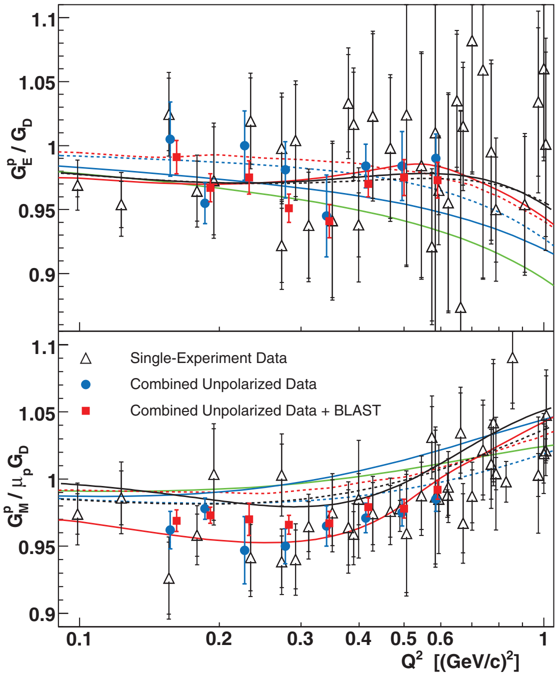

FIG. 2 (color). Compilation of world data on G_E^p/G_D and $G_M^p/\mu_p G_D$ at BLAST kinematics with (red) and without (blue) BLAST input, shown with total uncertainties. The results from single-experiment L-T separations [11,17,41–46] are shown with open symbols. The curves have the same meaning as in Fig. 1.

parametrizations by Friedrich and Walcher [2] and Kelly [40].

The impact of the BLAST results on the separated proton charge and magnetic form factors normalized to the dipole form factor $G_D = (1 + Q^2/0.71)^{-2}$ is illustrated in Fig. 2. In this figure, Rosenbluth extractions of G_E^p and G_M^p from single experiments [11,17,41–46] are presented as open triangles with statistical and total error bars, the systematic errors added in quadrature. The combined cross-section data [17,41–43,45–49], obtained from [45,50], were binned according to Table I to obtain a single L-T separation of G_E^p and G_M^p at each of the BLAST kinematics (blue circles). In comparison, the red squares show the form factors extracted by combining the unpolarized cross-section data and the measured form factor ratio from BLAST. Not only are the uncertainties reduced by a factor of 1.3–2.5, but also the negative correlation between G_E^p and G_M^p typical of L-T separations is greatly reduced. Details of the extraction will follow in a separate paper.

The extracted form factor ratio ($\mu_p G_E^p/G_M^p$) in our experiment is consistent with unity. However, the separated form factors may suggest a deviation from the dipole form below 1 (GeV/c)^2, particularly around $Q^2 \approx 0.3$ to 0.4 (GeV/c)^2, similar to what has been observed in the neutron magnetic form factor data [51]. Interestingly, the neutron electric form factor values [52] peak in a similar Q^2 region. A possible explanation for this observation could be a manifestation of the pion cloud at low momentum transfer [1,2]. However, more precise data and a more detailed theoretical understanding of the pion cloud effect are necessary before one can confirm and quantify such an effect.

We thank the staff at the MIT-Bates Linear Accelerator Center for the delivery of high quality electron beam and for their technical support. This research is supported in part by the U.S. Department of Energy and the National Science Foundation.

[1] A. Faessler, T. Gutsche, V. E. Lyubovitskij, and K. Pumsa-ard, Phys. Rev. D **73**, 114021 (2006).
[2] J. Friedrich and T. Walcher, Eur. Phys. J. A **17**, 607 (2003).
[3] G. A. Miller, Phys. Rev. C **66**, 032201(R) (2002).
[4] R. Alkofer *et al.*, Few-Body Syst. **37**, 1 (2005); A. Hoell *et al.*, Nucl. Phys. **A755**, 298 (2005).
[5] J. J. Kelly, Phys. Rev. C **66**, 065203 (2002).
[6] M. R. Schindler, J. Gegelia, and S. Scherer, Eur. Phys. J. A **26**, 1 (2005).
[7] H. H. Matevosyan, G. A. Miller, and A. W. Thomas, Phys. Rev. C **71**, 055204 (2005); R. G. Edwards, Nucl. Phys., Proc. Suppl. **B140**, 290 (2005); M. Göckeler *et al.*, Phys. Rev. D **71**, 034508 (2005).
[8] D. S. Armstrong *et al.*, Phys. Rev. Lett. **95**, 092001 (2005).
[9] C. E. Hyde-Wright and C. W. de Jager, Annu. Rev. Nucl. Part. Sci. **54**, 217 (2004); H. Gao, Int. J. Mod. Phys. E **12**, 1 (2003); **12**, 567(E) (2003).
[10] M. N. Rosenbluth, Phys. Rev. **79**, 615 (1950).
[11] R. C. Walker *et al.*, Phys. Rev. D **49**, 5671 (1994).
[12] L. Andivahis *et al.*, Phys. Rev. D **50**, 5491 (1994).
[13] T. W. Donnelly and A. S. Raskin, Ann. Phys. (N.Y.) **169**, 247 (1986).
[14] R. G. Arnold, C. E. Carlson, and F. Gross, Phys. Rev. C **23**, 363 (1981).
[15] M. Jones *et al.*, Phys. Rev. Lett. **84**, 1398 (2000); V. Punjabi *et al.*, Phys. Rev. C **71**, 055202 (2005); **71**, 069902(E) (2005).
[16] O. Gayou *et al.*, Phys. Rev. Lett. **88**, 092301 (2002).
[17] M. E. Christy *et al.*, Phys. Rev. C **70**, 015206 (2004).
[18] I. A. Qattan *et al.*, Phys. Rev. Lett. **94**, 142301 (2005).
[19] A. V. Belitsky, X. Ji, and Feng Yuan, Phys. Rev. Lett. **91**, 092003 (2003).
[20] J. P. Ralston and P. Jain, hep-ph/0207129; J. P. Ralston, R. V. Buniy, and P. Jain, hep-ph/0206063.
[21] G. A. Miller and M. R. Frank, Phys. Rev. C **65**, 065205 (2002).
[22] S. J. Brodsky, J. R. Hiller, D. S. Hwang, and V. A. Karmanov, Phys. Rev. D **69**, 076001 (2004).
[23] P. G. Blunden, W. Melnitchouk, and J. A. Tjon, Phys. Rev. Lett. **91**, 142304 (2003); Phys. Rev. C **72**, 034612 (2005); Y. C. Chen, A. Afanasev, S. J. Brodsky, C. E. Carlson, and M. Vanderhaeghen, Phys. Rev. Lett. **93**, 122301 (2004); A. V. Afanasev and N. P. Merenkov, Phys. Rev. D **70**, 073002 (2004).

[24] C. B. Crawford, Ph.D. thesis, Massachusetts Institute of Technology, 2005.
[25] A. T. Sindile, Ph.D. thesis, University of New Hampshire, 2006.
[26] B. Milbrath *et al.*, Phys. Rev. Lett. **80**, 452 (1998); **82**, 2221(E) (1999).
[27] S. Dieterich *et al.*, Phys. Lett. B **500**, 47 (2001).
[28] T. Pospischil *et al.*, Eur. Phys. J. A **12**, 125 (2001).
[29] O. Gayou *et al.*, Phys. Rev. C **64**, 038202 (2001).
[30] M. J. Alguard *et al.*, Phys. Rev. Lett. **37**, 1258 (1976).
[31] M. K. Jones *et al.*, Phys. Rev. C **74**, 035201 (2006).
[32] D. Cheever *et al.*, Nucl. Instrum. Methods Phys. Res., Sect. A **556**, 410 (2006); L. D. van Buuren *et al.*, Nucl. Instrum. Methods Phys. Res., Sect. A **474**, 209 (2001).
[33] D. Hasell *et al.*, The BLAST Experiment (to be published).
[34] A. Afanasev, I. Akushevich, and N. Merenkov, Phys. Rev. D **64**, 113009 (2001).
[35] C. Zhang, Ph.D. thesis, Massachusetts Institute of Technology, 2006); C. Zhang *et al.* (to be published).
[36] G. Holzwarth, Z. Phys. A **356**, 339 (1996).
[37] F. Cardarelli and S. Simula, Phys. Rev. C **62**, 065201 (2000); S. Simula, in *Proceedings of the Workshop on the Physics of Excited Nucleons* (World Scientific, Singapore, 2001), p. 135.
[38] E. L. Lomon, Phys. Rev. C **66**, 045501 (2002).
[39] H.-W. Hammer and Ulf-G. Meissner, Eur. Phys. J. A **20**, 469 (2004).
[40] J. J. Kelly, Phys. Rev. C **70**, 068202 (2004).
[41] T. Janssens *et al.*, Phys. Rev. **142**, 922 (1966).
[42] M. Goitein *et al.*, Phys. Rev. D **1**, 2449 (1970); L. E. Price *et al.*, Phys. Rev. D **4**, 45 (1971).
[43] C. Berger *et al.*, Phys. Lett. B **35**, 87 (1971).
[44] W. Bartel *et al.*, Nucl. Phys. **B58**, 429 (1973).
[45] F. Borkowski *et al.*, Nucl. Phys. **A222**, 269 (1974); Nucl. Phys. **B93**, 461 (1975).
[46] P. E. Bosted *et al.*, Phys. Rev. C **42**, 38 (1990).
[47] W. Bartel *et al.*, Phys. Rev. Lett. **17**, 608 (1966).
[48] S. Stein *et al.*, Phys. Rev. D **12**, 1884 (1975).
[49] M. I. Niculescu, Ph.D. thesis, Hampton University, 1999.
[50] J. Arrington, Phys. Rev. C **69**, 022201(R) (2004).
[51] W. Xu *et al.*, Phys. Rev. Lett. **85**, 2900 (2000); W. Xu *et al.*, Phys. Rev. C **67**, 012201 (2003).
[52] D. I. Glazier *et al.*, Eur. Phys. J. A **24**, 101 (2005); B. Plaster *et al.*, Phys. Rev. C **73**, 025205 (2006).